

# The Production of $^{52}\text{Fe}$ by Means of a Medium Energy Proton Accelerator

By Peter Smith-Jones <sup>1</sup>, Rolf Schwarzbach and Regin Weinreich

Paul Scherrer Institute, Würenlingen and Villigen, CH-5232 Villigen-PSI, Switzerland

*Dedicated to Professor G. Stöcklin on the occasion of his 60th birthday*

(Received November 17, 1989; revised January 3, 1990)

*Proton induced reactions / Radionuclide production /  $^{52}\text{Fe}$  / Thick target yield / PET radionuclide*

## Summary

The possible reactions induced by a 72 MeV proton beam for the formation of  $^{52}\text{Fe}$  are explored. For the most plausible target material of  $^{58}\text{Ni}$ , both production rates and thick target yields are given for the relevant iron radionuclides produced. Various chemical aspects are explored and a feasible chemical separation leading to the isolation of large amounts of no carrier added  $^{52}\text{Fe}$  is given. The overall yield and specific activity of  $^{52}\text{Fe}$  production by medium energy proton irradiation of a natural nickel target is more favorable than that of the reported Mn target.

## Introduction

Proton induced reactions for the large-scale production of positron emitting radionuclides, suitable for PET investigations, using proton beams in the region of 40–72 MeV, are being investigated as part of the research and development programme at the Paul Scherrer Institute (PSI). Since most of the lower energy proton induced reactions have been well documented [1–3], and since the lower energy part of the 72 MeV beam of the Injector II cyclotron is presently occupied in routine production purposes, the attention was focused on the upper energy range available (40–72 MeV), with the goal of a simultaneous bombardment of several targets.

Iron-52 ( $t_{1/2}$  8.27 h) is a useful radionuclide for studying the biochemistry of iron based compounds with potential applications in nuclear medicine (Ref. [4–5], and further references therein). Moreover  $^{52}\text{Fe}$  can be used as parent material in a radionuclide generator for the short-lived  $^{52\text{m}}\text{Mn}$  ( $t_{1/2}$  21.1m) [6–7]. Both  $^{52}\text{Fe}$  and  $^{52\text{m}}\text{Mn}$  are positron emitters and their decay characteristics [8] make them preferable to other iron and manganese radionuclides for quantitative PET studies.

Various production routes for  $^{52}\text{Fe}$  have been demonstrated and are summarized in Table 1. Despite the different production conditions cited in the literature and despite the questionable character of such comparisons at all, it seems that for a medium energy proton cyclotron the most favorable reaction reported is the  $^{55}\text{Mn}(p,4n)$ . However since the cross section for  $^{55}\text{Fe}$  production is an order of magnitude higher than that for  $^{52}\text{Fe}$  [9], this reaction gives a significant  $^{55}\text{Fe}$  impurity. This  $^{55}\text{Fe}$  impurity seems to be undesirable because of its long half life and associated patient radiation dose [10].

The proton bombardment of a nickel target to produce  $^{52}\text{Fe}$  has only been reported for proton energies above 200 MeV [11–13]. With respect to the formation of the three radionuclides  $^{52}\text{Fe}$ ,  $^{55}\text{Fe}$  [14, 15] and  $^{59}\text{Fe}$  [16], the proton energy range of the PSI injector cyclotrons (< 72 MeV) is covered by the nuclear reactions given in Table 2. Thus, these routes are occurring in a rather complex way, and the number of the reactions mentioned both in Table 2 and investigated in more detail by physical measurements is limited [17–22] and these measurements omit even the energy range under question. Moreover from the data given, it became apparent that the  $^{58}\text{Ni}(p,\alpha p2n)^{52}\text{Fe}$  reaction should reach its maximum cross section in the 60–65 MeV energy region. In addition to this the indirect formation of  $^{55}\text{Fe}$  will be limited by the 17.54 h half-life of the  $^{55}\text{Co}$  precursor, and in comparison the direct reactions leading to  $^{55}\text{Fe}$  are thought to be of a lower probability.

The separation of iron from nearby transition metals by anion or cation exchange chromatography using quarternary ammonium or sulphonic acid functional groups attached to a divinylbenzene styrene copolymer lattice and a medium of hydrochloric acid has been proven to be very effective [23]. In high concentrations of hydrochloric acid both iron(III) and gallium(III) form very stable anionic chloride complexes which are strongly retained by both types of resin. Other elements in the first row transition metal group show little or no absorption with cation exchange, but with anion exchange the selective elution of nickel, manganese, cobalt and iron has been demonstrated [24].

<sup>1</sup> On leave of absence from the National Accelerator Centre, Faure 7131, South Africa. Present address: Paul Scherrer Institute, Würenlingen and Villigen, CH-5232 Villigen-PSI, Switzerland.

Table 1. Production methods for  $^{52}\text{Fe}$ 

Target material		Nuclear reaction	Energy (MeV)	Production rate (a: $\mu\text{Ci}/\mu\text{Ah}$ , b: $\text{MBq}/\mu\text{Ah}$ , c: % of total)									Reference
				$^{52}\text{Fe}$		$^{55}\text{Fe}$			$^{59}\text{Fe}$				
				a	b	a	b	c	a	b	c		
Chromium	50 $\mu\text{m}$	$^{nat}\text{Cr}(\alpha, xn)$	30	3.3	0.12	0.46	0.017	14	ND	—	—	32	
Chromium	40 $\mu\text{m}$	$^{nat}\text{Cr}(\alpha, xn)$	30	3.8	0.14	0.43	0.016	11.3	ND	—	—	33, 34	
Chromium	40 $\mu\text{m}$	$^{nat}\text{Cr}(\alpha, xn)$	40	8.2	0.30	0.52	0.019	6.3	ND	—	—	33, 34	
Enriched $^{50}\text{Cr}$	40 $\mu\text{m}$	$^{50}\text{Cr}(\alpha, 2n)$	40	160	5.9	ND	—	—	ND	—	—	34	
Chromium	55 $\mu\text{m}$	$^{nat}\text{Cr}(\alpha, xn)$	65	3.8	0.14	0.19	0.007	5.0	ND	—	—	35	
$\text{Cr}_2\text{O}_7$	0.1 g/cm $^2$	$^{nat}\text{Cr}(\alpha, xn)$	85–53	30	1.11	ND	—	—	ND	—	—	36	
Chromium	7.2 $\mu\text{m}$	$^{nat}\text{Cr}(^3\text{He}, xn)$	23	0.7	0.03	0.002	0.00007	0.3	ND	—	—	37	
Chromium	40 $\mu\text{m}$	$^{nat}\text{Cr}(^3\text{He}, xn)$	30	13	0.48	0.032	0.0009	0.25	ND	—	—	34, 38	
Chromium	250 $\mu\text{m}$	$^{nat}\text{Cr}(^3\text{He}, xn)$	35	20	0.74	0.014	0.0005	0.07	ND	—	—	39, 40	
Chromium	40 $\mu\text{m}$	$^{nat}\text{Cr}(^3\text{He}, xn)$	40	50	1.85	0.036	0.0013	0.07	ND	—	—	34, 38	
Chromium	30 $\mu\text{m}$	$^{nat}\text{Cr}(^3\text{He}, xn)$	45	50	1.85	—	—	<0.001	ND	—	—	41	
$\text{MnO}_2$		$^{55}\text{Mn}(p, 4n)$	65	160	5.9	4.8	0.18	3	ND	—	—	42	
Manganese	2.6 g/cm $^2$	$^{55}\text{Mn}(p, 4n)$	70–50	200	7.4	1.4	0.05	0.7	ND	—	—	12	
Manganese		$^{55}\text{Mn}(p, 4n)$	60–44	600	22	2.7	0.1	0.45	ND	—	—	9	
Manganese	2.0 g/cm $^2$	$^{55}\text{Mn}(p, 4n)$	63–48	327	12.1	1.2	0.05	0.38	ND	—	—	30	
Nickel	0.5 mm	$^{nat}\text{Ni}(p, xn)$	200–198	120	4.4	2.4	0.09	2.0	0.2	0.008	0.17	11	
Nickel	6.5 mm	$^{nat}\text{Ni}(p, xn)$	588–580	700	26	23	0.85	3.3	3.5	0.13	0.5	11	
Nickel	8.0 mm	$^{nat}\text{Ni}(p, xn)$	800–790	134	5.0	ND	—	—	0.7	0.03	0.52	13	
Nickel	2.0 mm	$^{nat}\text{Ni}(p, xn)$	68–54	590	22	2.9	0.07	0.5	0.20	0.007	0.03	this work	
Nickel	1.9 g/cm $^2$	$^{nat}\text{Ni}(p, xn)$	63–48	491	18.1	10.1	0.37	2.0	0.24	0.008	0.05	30	
Ferrocene	1 g	$^{nat}\text{Fe}(\gamma, 2n)$	40	0.03	0.001	$3 \cdot 10^{-4}$	$10^{-5}$	1	ND	—	—	43	
Iron	1 g	$^{nat}\text{Fe}(\gamma, 2n)$	90	0.10	0.004	ND	—	—	ND	—	—	44	

ND: Not determined.

Table 2.  $Q$  values for the production of  $^{52}\text{Fe}$ ,  $^{55}\text{Fe}$ ,  $^{59}\text{Fe}$  and  $^{55}\text{Co}(\rightarrow ^{55}\text{Fe})$  by interaction of protons with nickel isotopes [45]

Reaction	% Abundance of target nuclide	$Q$ value (MeV)	Comments
$^{58}\text{Ni}(p, \alpha p 2n)^{52}\text{Fe}$	68.27	–30.5	Main route
$^{58}\text{Ni}(p, 3p 4n)^{52}\text{Fe}$	68.27	–54.4	
$^{60}\text{Ni}(p, \alpha p 4n)^{52}\text{Fe}$	26.11	–50.9	
$^{61}\text{Ni}(p, \alpha p 5n)^{52}\text{Fe}$	1.13	–58.7	
$^{62}\text{Ni}(p, \alpha p 6n)^{52}\text{Fe}$	3.59	–69.3	
$^{58}\text{Ni}(p, 3pn)^{55}\text{Fe}$	68.27	–25.4	Indirect
$^{60}\text{Ni}(p, \alpha pn)^{55}\text{Fe}$	26.11	–17.5	
$^{60}\text{Ni}(p, 3p 3n)^{55}\text{Fe}$	26.11	–45.8	
$^{61}\text{Ni}(p, \alpha p 2n)^{55}\text{Fe}$	1.13	–25.3	
$^{61}\text{Ni}(p, 3p 4n)^{55}\text{Fe}$	1.13	–53.6	
$^{62}\text{Ni}(p, \alpha p 3n)^{55}\text{Fe}$	3.59	–35.9	
$^{62}\text{Ni}(p, 3p 5n)^{55}\text{Fe}$	3.59	–64.2	
$^{64}\text{Ni}(p, \alpha p 5n)^{55}\text{Fe}$	0.91	–52.4	
$^{58}\text{Ni}(p, \alpha)^{55}\text{Co}$	68.27	–1.4	
$^{58}\text{Ni}(p, 2p 2n)^{55}\text{Co}$	68.27	–29.7	
$^{60}\text{Ni}(p, \alpha 2n)^{55}\text{Co}$	26.11	–21.7	
$^{60}\text{Ni}(p, 2p 4n)^{55}\text{Co}$	26.11	–50.0	
$^{61}\text{Ni}(p, \alpha 3n)^{55}\text{Co}$	1.13	–29.6	
$^{61}\text{Ni}(p, 2p 5n)^{55}\text{Co}$	1.13	–57.9	
$^{62}\text{Ni}(p, \alpha 4n)^{55}\text{Co}$	3.59	–40.2	
$^{62}\text{Ni}(p, 2p 6n)^{55}\text{Co}$	3.59	–68.5	
$^{64}\text{Ni}(p, 2p 8n)^{55}\text{Co}$	0.91	–56.7	
$^{61}\text{Ni}(p, 3p)^{59}\text{Fe}$	1.13	–18.1	Indirect
$^{62}\text{Ni}(p, 3pn)^{59}\text{Fe}$	3.59	–28.7	
$^{64}\text{Ni}(p, 3p 3n)^{59}\text{Fe}$	0.91	–45.2	
$^{64}\text{Ni}(p, \alpha pn)^{59}\text{Fe}$	0.91	–16.1	

Hence the purpose of this work was to measure the production functions for  $^{52}\text{Fe}$  for the energy region below 72 MeV as well as the formation of the contaminants  $^{55}\text{Fe}$  and  $^{59}\text{Fe}$ . In addition to this it was of paramount importance to produce  $^{52}\text{Fe}$  with a high specific activity (suitable for biological applications) so that a statement about the suitability of  $^{52}\text{Fe}$  produced by proton irradiation of natural nickel could be made.

## Experimental

### Targetry and irradiations

Irradiations were performed with both the 72 MeV Philips Injector I cyclotron and the newer Injector II cyclotron at the PSI. Circular discs from 13 mm to 30 mm in diameter were cut from 0.125 mm, 0.3 mm, 1.0 mm and 2.0 mm metallic nickel sheets (99.98% Goodfellow Metals, Cambridge, UK). Monitor foils of a corresponding diameter were cut from 0.13 and 0.457 mm metallic aluminum sheets (99.9% Goodfellow Metals, Cambridge, UK). The stacks were encased in aluminum cans 40 mm in diameter and up to 10 mm thick and bombarded at currents from 1  $\mu\text{A}$  to 40  $\mu\text{A}$  for maximum periods of up to 20 minutes in the existing radioisotope production vault using the off line  $^{123}\text{I}$  production beamline [25]. The target foils

were aligned perpendicular to the proton beam in such a way that successive foils received only the degraded beam coming from the preceding foil in the stack. The beam was focused to a diameter of 10–15 mm. In the experiments performed some 30 to 40% of the beam passed through the 13 mm foils and 99% of the beam was on target for the larger foils.

Several stacks of  $^{nat}\text{Ni}$  were bombarded, early experiments used alternate 0.125 mm Ni and 0.13 mm Al foils (13 mm diameter) to determine if product recoil was significant and in later experiments only 0.5 mm Al foils at 10 MeV intervals were used to check the position and scattering of the proton beam. Thick target yields used 1 mm and 2 mm thick foils (20–30 mm diameter) and a corresponding energy region of 67.8–53.9 MeV.

Beam currents were determined by analyzing the aluminum foils for the induced  $^7\text{Be}$ ,  $^{22}\text{Na}$  and  $^{24}\text{Na}$  activities, and by using the known cross section values [26]. Proton ranges were determined by using one of the more recently available proton range energy tables [27].

### Radionuclidic assays

An 84 cm<sup>3</sup> high purity germanium detector (n type) in conjunction with a 916 MCB card (EG & G ORTEC, Oak Ridge, Tennessee, USA) fitted in an IBM PC-AT was used to collect the  $\gamma$ -ray spectra. Analysis of the spectra was performed with the GELIGAM routine (EG & G ORTEC, Oak Ridge, Tennessee, USA). Calibration of the system in terms of both energy and detector efficiency was performed using various certified point sources of reference date 25/6/86 (Laboratoire de Métrologie des Rayonnements Ionisants, Gif-sur-Yvette, France). Foils were assayed at distances of 35 to 5 cm from the detector at times ranging from EOB + 8 h to EOB + 90 d depending on the activity induced therein. The “dead time” of the counting system was not allowed to exceed 20%.

Iron-55 activities were determined by isolating the iron isotopes from any other radionuclides and the target matrix, after a decay time of 90 days, by cation exchange chromatography. The foils were dissolved in 10 M HCl and 1  $\mu\text{g}$  of Fe(III) carrier added. The solution obtained was oxidized using  $\text{H}_2\text{O}_2$ , adjusted to 8 M HCl and then loaded onto a 5 ml column of AG50-X8 resin (H form, 100–200 mesh). The nickel target material as well as induced cobalt and manganese activities were easily eluted on loading and further washing with 20 ml of 8 M HCl removed traces. Iron was stripped from the column using 4.0 M HCl and excess acid removed. The sample remaining was dissolved in 0.05 M HCl and was counted by means of Liquid Scintillation Counting as a 10% aqueous cocktail in “Instagel” (a standard  $^{55}\text{Fe}$  reference solution was obtained from Amersham International plc, Buckinghamshire, UK).  $^{59}\text{Fe}$  was determined in the isolated iron fraction prior to LSD counting. A known

amount of  $^{52}\text{Fe}$  was similarly separated from a simulated target matrix and  $\gamma$ -ray analysis showed the separation to be quantitative.

The errors involved in the radionuclidic assays were estimated by obtaining the sum of all the contributing errors.

The energy calculations were estimated to be within 3.4% of the energy window chosen and were determined using the following errors; incident proton energy (0.1%), proton range energy values (1.0%), target density (1.0%) and proton straggling (1.3%). The well known straggling of the proton energy by interaction with materials [27] seems to be proportional (for the energy range investigated) to the target density (atoms/cm<sup>2</sup>) and for the degradation of a 70 MeV beam to 60, 50 and 40 MeV in a nickel target it was estimated to be 0.7, 1.5 and 2.3 MeV, respectively.

The beam current determinations were estimated to be within 10.8% of the values obtained and were determined from the following errors: target density (1%), proton range energy values (1%), cross-section measurements (3.0%), standard calibration sources (2.6%), extrapolated detector efficiencies (1.5%), counting geometries (0.2%), decay corrections (0.3% for  $^{22}\text{Na}$  only), gamma ray abundances (0.4%), photopeak integrations (1%). Recoil losses were considered to be negligible.

The production yields were estimated to be within 16% of the values obtained for  $^{52}\text{Fe}$  (16% for  $^{55}\text{Fe}$  (via  $^{55}\text{Co}$ ), 29% for  $^{55}\text{Fe}$  and 19% for  $^{59}\text{Fe}$ ) and were determined from the following errors: target density (1%), proton range energy values (1%), cross-section determination (10.8%), extrapolated detector efficiencies (1.5%), counting geometries (0.2%), decay corrections (0.1%), gamma ray abundances (0.4%), photopeak integrations (1% for  $^{52}\text{Fe}$ , 1% for  $^{55}\text{Co}$  and 5% for  $^{59}\text{Fe}$ ) and, for  $^{55}\text{Fe}$ , LSD counting uncertainty (15%).

### Radiochemistry

Cation exchange chromatography is an exceedingly good tool for the separation of iron from all non-ferrous first row transition metals but it necessitates the use of concentrated acids. Iron is an impurity found in most chemical reagents and as a result of this relatively large amounts of carrier iron can be introduced by this technique. Anion exchange on the other hand uses less concentrated reagents for the removal of non-ferrous cations.

The anion exchange separation of the first nickel targets (25 mm  $\times$  2 mm) was performed by initially dissolving the metal in 100 ml 7 M  $\text{HNO}_3$ . The solution obtained was evaporated down to near dryness and 60 ml 6 M HCl were added. The cold solution obtained was loaded onto a 25 ml column of Dowex 1-X8 (125 mm  $\times$  15 mm, 100–200 mesh, prewashed with 200 ml 0.1 M HCl and equilibrated with 6 M

**Table 3.** Thick target yields for  $^{52}\text{Fe}$  and radionuclidic contaminants

Energy window (MeV)	Production rates ( $\text{kBq}/\mu\text{Ah}$ )				Impurities (%)		
	$^{52}\text{Fe}$	$^{55}\text{Fe}$	$^{55}\text{Fe}$ (via $^{55}\text{Co}$ )	$^{59}\text{Fe}$	$^{55}\text{Fe}$	$^{55}\text{Fe}$ (via $^{55}\text{Co}$ )	$^{59}\text{Fe}$
69.1–67.6	2770	18.0	15.1	0.73	0.65	0.55	0.026
67.6–66.2	2860	15.6	14.8	0.69	0.54	0.52	0.024
66.2–64.7	2930	12.0	14.1	0.71	0.46	0.48	0.024
64.7–63.3	2870	13.4	14.4	0.74	0.46	0.50	0.026
63.3–61.8	2750	13.9	15.0	0.67	0.50	0.55	0.024
61.8–60.4	2620	13.3	15.0	0.65	0.51	0.57	0.024
60.4–58.9	2480	12.9	14.1	0.72	0.52	0.57	0.029
58.9–57.5	2360	11.2	14.5	0.62	0.47	0.61	0.026
57.5–56.0	2160	9.23	15.1	0.65	0.43	0.70	0.030
56.0–54.6	1820	8.83	14.6	0.85	0.48	0.81	0.047
54.6–53.1	1470	9.52	13.8	0.78	0.65	0.94	0.035
53.1–51.6	1180	10.5	13.2	0.56	0.89	1.12	0.047
51.6–50.2	980	11.1	12.6	0.45	1.13	1.29	0.046
50.2–48.7	750	10.5	11.7	0.44	1.40	1.56	0.058
48.7–47.3	376	8.59	9.67	0.37	2.28	2.57	0.099
47.3–45.8	52	6.78	7.55	0.31	13.04	14.52	0.59

HCl). Manganese, cobalt and nickel were eluted with 400 ml of 3 M HCl at a flow rate of 1.7 ml/min. Finally  $^{52}\text{Fe}$  was eluted with 50 ml of 0.1 M HCl at a flow rate of 1.7 ml/min. Later improvements in the targetry reduced the target size to  $18 \times 18 \times 1$  mm which reduced the volume of 7 M  $\text{HNO}_3$  required to dissolve the target to 80 ml. The solution obtained was then treated as above.

Determination of active components was performed using the aforementioned HPGE counting system after appropriate waiting times. Determination of carrier iron concentrations was performed by the standard thiocyanate method [28] and a Hewlett Packard 8452A diode array spectrophotometer.

## Results and discussion

### Production rates

Figure 1 and Table 3 give the production rates and thick target yields, respectively, observed in this study for  $^{52}\text{Fe}$ ,  $^{55}\text{Fe}$  and  $^{59}\text{Fe}$  from a natural nickel target. The shapes of the curves are generally as expected considering the  $Q$  values for the numerous reactions possible in this energy region. The agreement with the only other data set by Steyn *et al.* [30] is fairly good except for the reported levels of directly produced  $^{55}\text{Fe}$ , which they report as being about twice as high as the present work, but this could possibly be due to their chemical separation technique which, in practice, results in a very poor decontamination factor for cobalt and vanadium.

Figure 2 shows the yields of  $^{52}\text{Fe}$  measured in this study and three others. Production rates obtained from the work of Tanaka *et al.* [17] and Dmitriev [31] come from cross section measurements and thick target yields (1 MeV window) for the reaction of 56 and 60 MeV protons with enriched  $^{58}\text{Ni}$ . These two

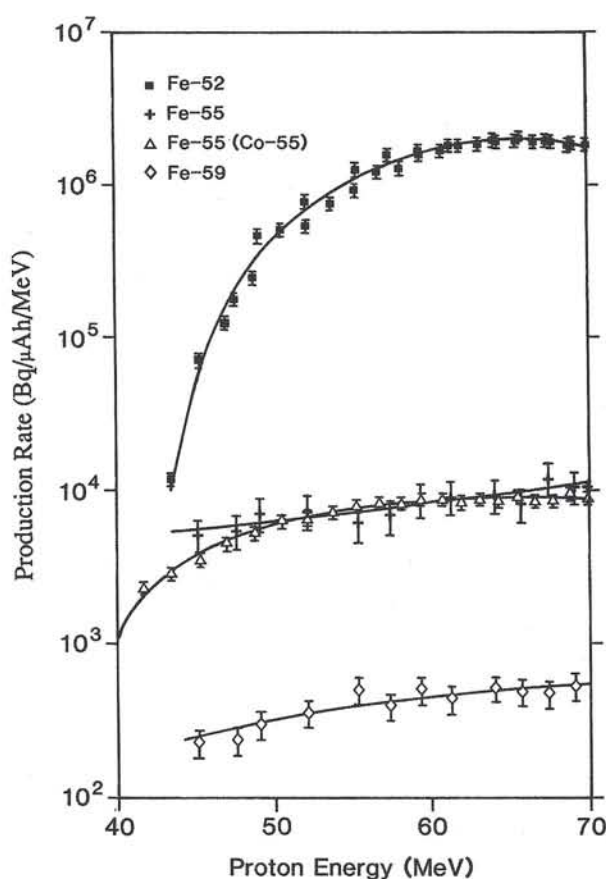


**Fig. 1.** Production rates for  $^{52}\text{Fe}$ ,  $^{55}\text{Fe}$  and  $^{59}\text{Fe}$  from the 72 MeV proton bombardment of natural nickel. ( $^{55}\text{Fe}(^{55}\text{Co})$  indicates indirectly produced  $^{55}\text{Fe}$  and is based on  $^{55}\text{Co}$  measurements.)

works can be directly compared to our work because the contribution from  $^{60}\text{Ni}$  can be considered to be negligible in comparison. Data obtained from Steyn *et al.* [30] however relates to tabulated production rates for 100 MeV and 66 MeV protons on  $^{\text{nat}}\text{Ni}$ . The



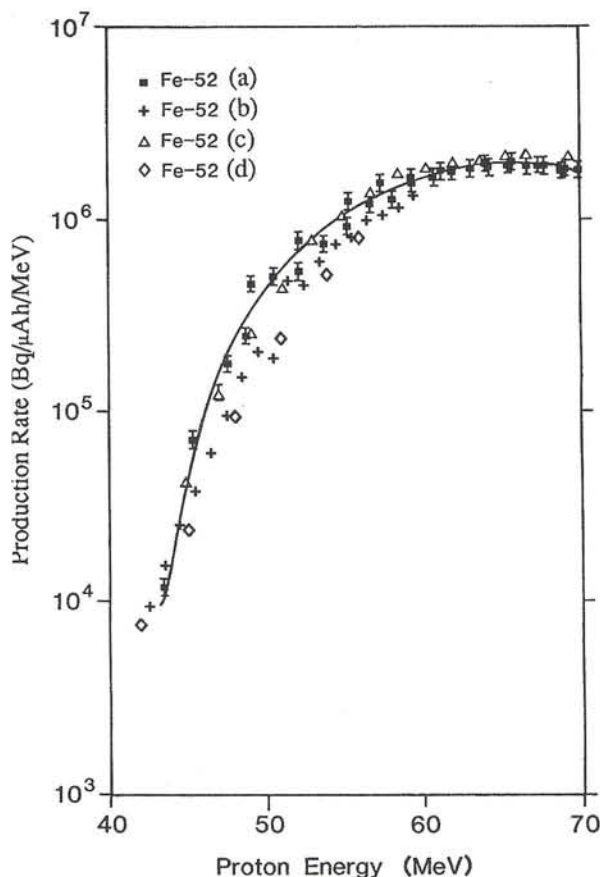


Fig. 2. Comparison of various reported production rates for  $^{52}\text{Fe}$  from the proton bombardment of nickel. (a) This work, (b) Ref. 31, (c) Ref. 30, (d) Ref. 17.

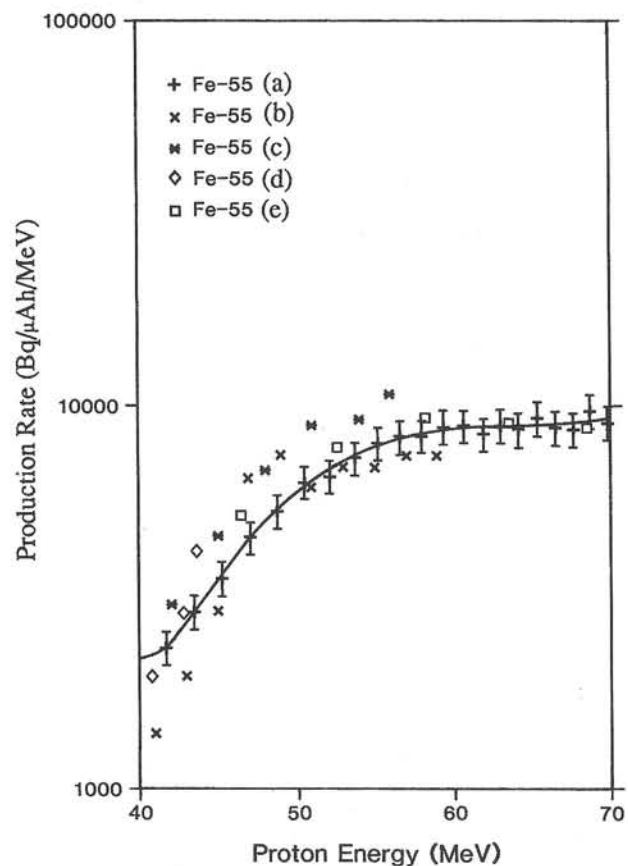


Fig. 3. Comparison of various production rates for indirectly produced  $^{55}\text{Fe}$  based on the reported production rates for  $^{55}\text{Co}$ . (a) This work, (b) Ref. 31, (c) Ref. 17, (d) Ref. 18, (e) Ref. 30.

agreement with Steyn *et al.* [30], about 10% lower at higher energies, is good considering that their in house determination of the  $^{27}\text{Al}(p,xn)^{22/24}\text{Na}$  reactions are some 10% out from those given by Grütter [26] and used in this work. The values obtained from Tanaka *et al.* [17] and Dmitriev [31] however are consistently lower. In the region 60–70 MeV the curve is fairly flat, but a maximum is observed at about 65 MeV.

Figure 3 shows the comparison of our data with four other data sets for the indirect production of  $^{55}\text{Fe}$  via decay of  $^{55}\text{Co}$ . As in the previous figure the production rates of Tanaka *et al.* [17] were derived from cross section measurements on  $^{58}\text{Ni}$  as were those of Michel *et al.* [18] except that they used 45 MeV protons on  $^{nat}\text{Ni}$ . Also the data given by Dmitriev [31] is derived from thick target data (2 MeV windows) as is that of Steyn *et al.* [30]. In general the agreement is quite good (except for Tanaka *et al.* [17]) if one considers the effect of proton straggling for the higher energy degradation produced in the larger foil stacks.

From the point of view of radioisotopic purity the best production route demonstrated for the production of  $^{52}\text{Fe}$  is the  $^{nat}\text{Cr}(^3\text{He}, xn)$ , but the low production rates (ca. 50  $\mu\text{Ci}/\mu\text{Ah}$ ) would place unacceptable demands on beam time. The manganese target and proton irradiation has been shown to give

production rates comparable to those of a nickel target and with a similar  $^{55}\text{Fe}$  contamination level.

### Large scale production

Some 20 production runs of  $^{52}\text{Fe}$  for in house PET experiments and for  $^{52}\text{Fe}/^{52\text{m}}\text{Mn}$  generator studies have resulted in a yield some 90% of the theoretical value. A  $\gamma$ -spectrum taken from a sample of  $^{52}\text{Fe}$  some 250 hours after production revealed only the expected decay product  $^{52}\text{Mn}$  and the byproduct  $^{59}\text{Fe}$ . Estimation of the most expected radionuclidic impurities of  $^{56}\text{Co}$ ,  $^{58}\text{Co}$  and  $^{56}\text{Ni}$  were all less than  $1 \cdot 10^{-6}\%$  compared to the initial  $^{52}\text{Fe}$  activity.

Initially, in our routine production runs, we obtained iron levels typically in the 80–90  $\mu\text{g}$  range for one batch production regardless of activity produced. Further analysis revealed that the nickel target (8.8 g) contained 60–65  $\mu\text{g}$  of iron and the remainder 20–25  $\mu\text{g}$  was coming from the reagents used (all Merck Pro Analysis grade).

The only other data for carrier iron levels were given by Steyn *et al.* [30] as 2170  $\mu\text{g}$  for a manganese target and 120  $\mu\text{g}$  for a nickel target. These levels are clearly unacceptable for iron studies, particularly for

smaller animals since the natural iron balance will be perturbed (in humans the levels of iron bound to transferrin are around 1 mg/l whole blood [28]).

An alternative to longer bombardment times is to use purer materials and, since recently a commercial supplier (Goodfellow) has included a high purity nickel (stated as <2 ppm Fe but found to be 1 ppm) in their catalogue, we have altered our targetry to accommodate a smaller target (18 × 18 × 1 mm). This has resulted in reducing the production rate by a factor of 2 but iron levels are now about 5 µg with 3.4–3.6 µg coming from the nickel and about 1.5 µg coming from the chemical processing (Merck Suprapur grade reagents). This enables  $^{52}\text{Fe}$  of a suitable specific activity for protein labelling (10 mCi/µg) to be produced with only a 4 hour bombardment.

### Conclusion

The bombardment of a nickel target with 72 MeV protons has been shown to be the best option for  $^{52}\text{Fe}$  production regardless of whether it is to be used for labelling purposes or in the  $^{52}\text{Fe}/^{52\text{m}}\text{Mn}$  generator system. The yield of  $^{52}\text{Fe}$  is higher than for other reported reactions and the formation of  $^{55}\text{Fe}$  is comparable to that from the manganese target. The physical properties of nickel make it ideally suited to direct water cooling and consequently higher beam currents may be used. Since nickel is relative easy to refine, it is available in a highly pure metallic form which makes it more readily suited to the production of  $^{52}\text{Fe}$  with a high specific activity.

### Acknowledgements

The authors would like to thank Mr. R. Maag and Mr. J. Jegge for their valuable assistance in target preparation and irradiation, Dr. H. W. Reist for his advice concerning proton energy degradation and energy straggling, Mr. H. Hügli for the analysis of  $^{55}\text{Fe}$  and the National Accelerator Centre of South Africa for allowing P. M. Smith-Jones to take leave of absence.

### References

- Waters, S. L., Silvester, D. J.: Inorganic Cyclotron Radionuclides. *Radiochim. Acta* **30**, 163–173 (1982).
- Qaim, S. M.: Nuclear Data Relevant to Cyclotron Produced Short-lived Medical Radioisotopes. *Radiochim. Acta* **30**, 147–162 (1982).
- Qaim, S. M.: Cyclotron Production of Generator Radionuclides. *Radiochim. Acta* **41**, 111–117 (1987).
- Knospe, W. H., Rayudu, G. V. S., Cardello, M., Friedman, A. M., Fordham, E. W.: Bone Marrow Scanning with  $^{52}\text{Fe}$  ( $^{52}\text{Fe}$ ). Regeneration and Extension of Marrow after Ablative Doses of Radiotherapy. *Cancer* **37**, 1432 (1976).
- Chauncey, D. M., Schelbert, H. R., Halpern, S. E., Delano, F., McKegney, M. L., Ashburn, W. L., Hagan, P. L.: Tissue Distribution Studies with Radioactive Manganese: A Potential Agent for Myocardial Imaging. *J. Nucl. Med.* **18**, 933–936 (1977).
- Lambrecht, R. M.: Radionuclide Generators. *Radiochim. Acta* **34**, 9–24 (1983).
- Herscheid, J. D. M., Vos, C. M., Hoekstra, A.: Manganese-52m for Direct Application: A New  $^{52}\text{Fe}/^{52\text{m}}\text{Mn}$  Generator Based on a Hydroxamate Resin. *Int. J. Appl. Radiat. Isot.* **34**, 883–886 (1983).
- Beene, J. R.: Nuclear Data Sheets for A = 52. *Nucl. Data Sheets* **25**, 235–374 (1978).
- Suzuki, K.: Production of  $^{52}\text{Fe}$  by the  $^{55}\text{Mn}(p,4n)^{52}\text{Fe}$  Reaction and Milking of  $^{52\text{m}}\text{Mn}$  from  $^{52}\text{Fe}$ . *Radioisotopes (Tokyo)* **34**, 537–542 (1985).
- Robertson, J. S., Price, R. R., Budinger, T. F., Fairbanks, V. F., Pollycove, M.: MIRD Dose Estimate Report No. 11. Radiation Absorbed Doses from Iron-52, Iron-55 and Iron-59 Used to Study Ferrokinetics. *J. Nucl. Med.* **24**, 339–348 (1983).
- Sodd, V. J., Scholz, K. L., Blue, J. W.:  $^{52}\text{Fe}$  Production for Medical Use from 588-MeV-Proton Irradiation of Mn, Co, Ni and Cu Targets. *Med. Phys.* **1**, 25–28 (1974).
- Ku, T. H., Richards, P., Stang, L. G., Prach, T.: Preparation of  $^{52}\text{Fe}$  and its Use in a  $^{52}\text{Fe}/^{52\text{m}}\text{Mn}$  Generator. *Radiology* **132**, 475–477 (1979).
- Steinkruger, F. J., Bentley, G. E., O'Brien, H. A., Ott, M. A., Steurer, F. H., Taylor, W. A., Barnes, J. W.: *Production and Recovery of Large Quantities of Radionuclides for Nuclear Medicine Generator Systems*. ACS Symposium Series 241 (F. F. Knapp and T. A. Butler, eds.) ACS, Washington DC (1984).
- Campbell, J. L., Perujo, A., Teesdale, W. J., Millman, B. M.:  $K\alpha$ ,  $K\beta$ , and Irradiated Auger Photon Intensities in K X-ray Spectra from Atoms in the  $20 \leq Z \leq 40$  Region. *Phys. Rev. A*, **33**, 2410–2417 (1986).
- Debertin, K., Furnari, J. C., Walz, K. F.: Standard Sources for the Efficiency Calibration of Photon Detectors in the Energy Range from 5 to 40 keV. *Int. J. Appl. Radiat. Isot.* **36**, 977–980 (1985).
- Andersson, P., Ekstrom, L. P., Lyttkens, J.: Nuclear Data Sheet for A = 59. *Nucl. Data Sheets* **39**, 641–740 (1983).
- Tanaka, S., Furukawa, F., Chiba, M.: Nuclear Reactions of Nickel with Protons up to 56 MeV. *J. Inorg. Nucl. Chem.* **34**, 2419–2426 (1972).
- Michel, R., Weigel, H., Herr, W.: Proton induced Reactions on Nickel with Energies Between 12 and 45 MeV. *Z. Physik A*, **286**, 393–400 (1978).
- Grant, P. M., O'Brien, H. A., Bayhurst, B. P., Gilmore, J. S., Prestwood, R. J., Whipple, R. E., Wanek, P. M.: Spallation Yields of Fe-52, Cu-67, Ga-67 and Tl-201 from Reactions of 800 MeV Protons with Ni, As, Pb, and Bi Targets. *J. Lab. Comp. Radiopharm.* **16**, 212 (1979).
- Sadler, M. E., Singh, P. P., Jastrzebski, J.: Interaction of 80–164 MeV Protons with Nickel Isotopes. *Phys. Rev. C*, **21**, 2303–2321 (1980).
- Jastrzebski, J., Karwowski, H. J., Sadler, M., Singh, P. P.: Recoil Ranges of Nuclei Produced in the Interaction of 80–164 MeV Protons with Ni. *Phys. Rev. C*, **22**, 1443–1453 (1980).
- Asano, T., Asano, Y., Iguchi, Y., Kudo, H., Mori, S., Noguchi, M., Takada, Y., Hirabayashi, H., Ikeda, H., Katoh, K., Kondo, K., Takasaki, M., Tominaka, T., Yamamoto, A.: Target Dependence of Charge Distributions in Spallation Reactions of Medium Mass Nuclei with 12 GeV Protons. *Phys. Rev. C*, **28**, 1718–1724 (1983).
- Saito, N.: Selected Data on Ion Exchange Separations in Radioanalytical Chemistry. *Pure Appl. Chem.* **56**, 523–539 (1984).
- Kraus, K. A., Moore, G. E.: Absorption of Divalent Transition Elements from Manganese to Zinc. *J. Am. Chem. Soc.* **75**, 1460–1462 (1953).
- Weinreich, R., Reist, H. W., Maag, R., Oehniger, H.: Production of Short-Lived Positron Emitters Using a Split Beam of 72 MeV Protons. *Nucl. Med.* **26**, 196–197 (1987).
- Grütter, A.: Excitation Functions for Radioactive Isotopes Produced by Proton Bombardment of Cu and Al in the

- Energy Range of 16 to 70 MeV. Nucl. Phys. A383, 98–108 (1982).
27. Janni, J. F.: Proton Range Energy Tables, 1 keV–10 GeV. At. Data Nucl. Data Tables, 27, 341–529 (1982).
  28. Hughes, E. R.: Human Iron Metabolism. In: *Metal Ions in Biological Systems, Volume 7. Iron in Model and Natural Compounds*. (H. Sigel, ed.), Marcel Dekker Inc., New York (1974).
  29. Furman, N. H.: *Standard Methods of Chemical Analysis*. 6th ed., D. Van Nostrand Company Inc. Princeton, New Jersey (1962).
  30. Steyn, G. F., Mills, S. J., Nortier, F. M., Simpson, B. R. S., Meyer, B. R.: Production of  $^{52}\text{Fe}$  via Proton Induced Reactions on Manganese and Nickel. 41, 315–326 (1990).
  31. Dmitriev, P. P.: Radionuclide Yield in Reactions with Protons, Deuterons, Alpha Particles and Helium-3. International Nuclear Data Committee, IAEA Nuclear Data Section, INDC(CCP)-263/G+CN+SZ, Vienna 1986.
  32. Thakur, M. L., Nunn, A. D., Waters, S. L.: Iron-52: Improving its Recovery from Cyclotron Targets. Int. J. Appl. Radiat. Isot. 22, 481–483 (1971).
  33. Akiha, F., Aburai, T., Nozaki, T., Murakami, Y.: Yield of  $^{52}\text{Fe}$  for the Reactions of  $^3\text{He}$  and  $\alpha$  on Chromium. Radiochim. Acta 18, 108 (1972).
  34. Akiha, F., Murakami, Y.: Excitation Curves and Thick Target Yield Curves of  $^{52}\text{Fe}$ ,  $^{55}\text{Fe}$ ,  $^{56}\text{Mn}$ ,  $^{48}\text{Cr}$ ,  $^{49}\text{Cr}$ ,  $^{51}\text{Cr}$  and  $^{48}\text{V}$  for the  $(\text{Cr} + ^3\text{He})$  Reactions on Natural Chromium. Nippon Kagaku Kaishi 8, 1416–1421 (1972).
  35. Yano, Y., Anger, H. O.: Production and Chemical Processing of  $^{52}\text{Fe}$  for Medical Use. Int. J. Appl. Radiat. Isot. 16, 153–156 (1965).
  36. Cavallero, A., Cogneau, M. A., Apers, D. J.: Cross Sections and Excitation Functions of 40 to 110 MeV  $\alpha$ -Particle Induced Reactions in Natural Chromium. Radiochim. Acta 24, 11–14 (1977).
  37. Dahl, J. R., Tilbury, R. S.: The Use of a Compact, Multi-particle Cyclotron for the Production of  $^{52}\text{Fe}$ ,  $^{67}\text{Ga}$ ,  $^{111}\text{In}$  and  $^{123}\text{I}$  for Medical Purposes. Int. J. Appl. Radiat. Isot. 23, 431–437 (1972).
  38. Akiha, F.: Studies on Excitation Curves and Thick Target Yield Curves of  $^{52}\text{Fe}$ ,  $^{55}\text{Fe}$ ,  $^{56}\text{Mn}$ ,  $^{49}\text{Cr}$ ,  $^{51}\text{Cr}$  and  $^{48}\text{V}$  Formed by Bombardment of  $\alpha$  Particles on Natural Chromium. Nippon Kagaku Kaishi 9, 1664–1669 (1972).
  39. Rayudu, G. V. S., Shirazi, S. P. H., Fordham, E. W.: Comparison of the Use of  $^{52}\text{Fe}$  and  $^{111}\text{In}$  for Hemopoietic Marrow Scanning. Int. J. Appl. Radiat. Isot. 24, 451–454 (1973).
  40. Atcher, R. W., Friedman, A. M., Huizenga, J. R.: Production of  $^{52}\text{Fe}$  for use in a Radionuclide Generator System. Int. J. Nucl. Med. Biol. 7, 75–78 (1980).
  41. Greene, M. W., Lebowitz, E., Richards, P., Hillman, M.: Production of  $^{52}\text{Fe}$  for Medical Use. Int. J. Appl. Radiat. Isot. 21, 719–723 (1970).
  42. Saha, G. B., Farrer, P. A.: Production of  $^{52}\text{Fe}$  by the  $^{55}\text{Mn}(p,4n)^{52}\text{Fe}$  Reaction for Medical Use. Int. J. Appl. Radiat. Isot. 22, 495–498 (1971).
  43. Lindner, L., Kapteyn, J. C.: A Novel Way to Produce  $^{52}\text{Fe}$ . Proc. 15th Int. Ann. Meeting, Eur. Soc. of Nucl. Med., Groningen, The Netherlands (1977).
  44. Lindner, L., Kapteyn, J. C.:  $^{54}\text{Fe}(\gamma,2n)^{52}\text{Fe}$  Induced Szilard-Chalmers Effect in Ferrocene and Ferricinium Picrate. Radiochim. Acta 26, 97–101 (1979).
  45. Keller, K. A., Lange, J., Münzel, H.:  $Q$  Values and Excitation Functions for Charged Particle Induced Nuclear Reactions. In: *Landolt-Börnstein Neue Serie 1/5a* (K. H. Hellwege, ed.) Springer-Verlag, Berlin (1973).

